RESEARCH ARTICLE | MAY 08 2024

Electron irradiation effects on the optical properties of Hf- and Zn-doped β-Ga_2O_3

Special Collection: Defects in Semiconductors 2024

Cassandra Remple ; Jesse Huso ; Marc H. Weber ; John S. McCloy ; Matthew D. McCluskey

J. Appl. Phys. 135, 185702 (2024)
https://doi.org/10.1063/5.0196824

Journal of Applied Physics ARTICLE pubs.aip.org/aip/jap

Electron irradiation effects on the optical properties of Hf- and Zn-doped β-Ga_2O_3

Cite as: J. Appl. Phys. **135**, 185702 (2024); doi: 10.1063/5.0196824
Submitted: 9 January 2024 · Accepted: 19 April 2024 ·
Published Online: 8 May 2024

View Online Export Citation CrossMark

Cassandra Remple,[1] Jesse Huso,[2] Marc H. Weber,[3,4] John S. McCloy,[1,3] and Matthew D. McCluskey[1,2,4,a)]

AFFILIATIONS

[1]Materials Science and Engineering Program, Washington State University, Pullman, Washington 99164-2711, USA
[2]Klar Scientific, 1615 NE Eastgate Blvd., Unit G, Ste. 3E, Pullman, Washington 99163-5300, USA
[3]Institute of Materials Research, Washington State University, Pullman, Washington 99164-2711, USA
[4]Department of Physics and Astronomy, Washington State University, Pullman, Washington 99164-2814, USA

Note: This paper is part of the special topic, Defects in Semiconductors 2024.
[a)]**Author to whom correspondence should be addressed:** mattmcc@wsu.edu

ABSTRACT

Optical and electrical properties of Hf- and Zn-doped β-Ga_2O_3 samples, which are *n*-type and insulating, respectively, were altered via high-energy electron irradiation at 2.5 or 0.5 MeV. The β-Ga_2O_3:Hf samples irradiated with 2.5 MeV electrons experienced a color change from blue to yellow and a large drop in conductivity, attributed to the creation of gallium vacancies, which compensate donors. This irradiation resulted in the absence of free carrier absorption and the presence of Cr^{3+} photoluminescence (PL). PL mapping prior to irradiation revealed optically active ZnO precipitates that formed during the growth of β-Ga_2O_3:Zn. These precipitates have a 384 nm (3.23 eV) stacking fault emission in the core; in the outer shell of the precipitate, the PL blue-shifts to 377 nm (3.29 eV) and a broad defect band is observed. After 0.5 MeV electron irradiation, the defect band broadened and increased in intensity. The blue PL band (435 nm) of β-Ga_2O_3 was enhanced for both Hf- and Zn-doped samples irradiated with 0.5 MeV. This enhancement is correlated with an increase in oxygen vacancies.

I. INTRODUCTION

The beta phase of gallium oxide has been studied as a promising ultrawide bandgap semiconductor, with a bandgap of about 4.8 eV.[1] Monoclinic β-Ga_2O_3 has been studied for applications in high-power electronics,[2–4] solar-blind photodetectors,[5] radiation detectors/scintillators,[6–12] and thermal actuators.[13] Understanding defects in this material could lead to improvements in device properties.

In this work, the samples were exposed to high-energy electron irradiation. This method has been used to investigate native defects, primarily V_{Ga} and V_O, in β-Ga_2O_3.[14–16] Irradiation by electrons with energies in the MeV range produces well-defined, stable Frenkel vacancy–interstitial pairs because the small electron mass allows for minimal transfer of energy to the heavier nuclei, with just enough energy to eject an atom from its lattice site.[14,17] This is in contrast to protons or heavier particles,[18,19] where a larger amount of energy is transferred. In those cases, a similar first collision damage process can also generate a cascade of secondary events, leading to more complex and extended defects.[14,20–22]

Electron irradiations of 2.5 and 0.5 MeV were performed. At these energies, electrons penetrate through the bulk of the sample (2.5 MeV) or ~1 mm into the sample (0.5 MeV).[16,23] Prior work has estimated the energy displacement parameters for oxygen and gallium to be ~25 eV.[16,24] Simulations indicate that the cross section for oxygen vacancy creation by 0.5 MeV electrons is much higher than that for gallium due to the higher maximum energy transfer to the lighter oxygen atom.[14,16] From those studies, it follows that primarily oxygen vacancies should be formed with 0.5 eV energy irradiation. The higher energy 2.5 MeV irradiation, in contrast, is expected to displace both oxygen and gallium.[15,16]

Hf- and Zn-doped samples were studied. These were selected because they are *n*-type and insulating materials, respectively.

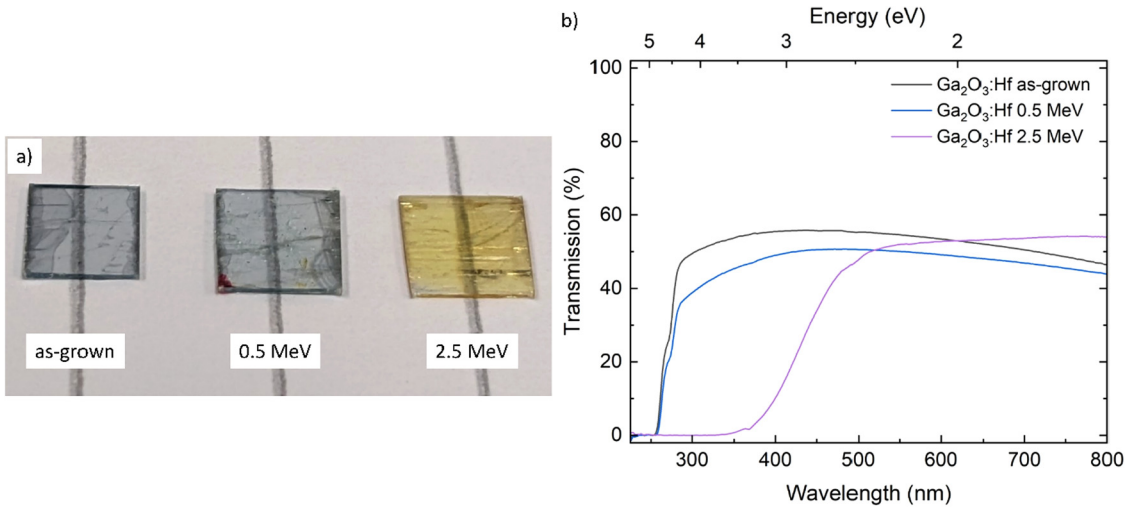

FIG. 1. (a) Image showing color change of Hf-doped β-Ga_2O_3 as-grown, 0.5 MeV, and 2.5 MeV irradiated samples. (b) UV-Vis transmission spectra of the samples.

Photoluminescence (PL) was studied before and after electron irradiation. Specifically, we examined the UV/blue band, which may relate to V_O as well as Cr^{3+} emissions. Cr^{3+} serves as a probe for the Fermi level and defect behavior in the material.[25,26] Peres *et al.*[22] reported that Cr^{3+} PL could be enhanced due to Fermi level pinning caused by proton radiation effects. The intensity of Cr^{3+} PL in β-Ga_2O_3 depends on the conductivity of the samples and, therefore, is affected by the defects present in the material.

Cr is a common unintentional dopant in β-Ga_2O_3 and is typically in the Cr^{3+} state.[27,28] Cr^{3+} preferentially occupies the octahedral Ga(II) site and has d^3 electronic configuration.[29,30] Crystal field splitting results in multiple energy levels, which give rise to

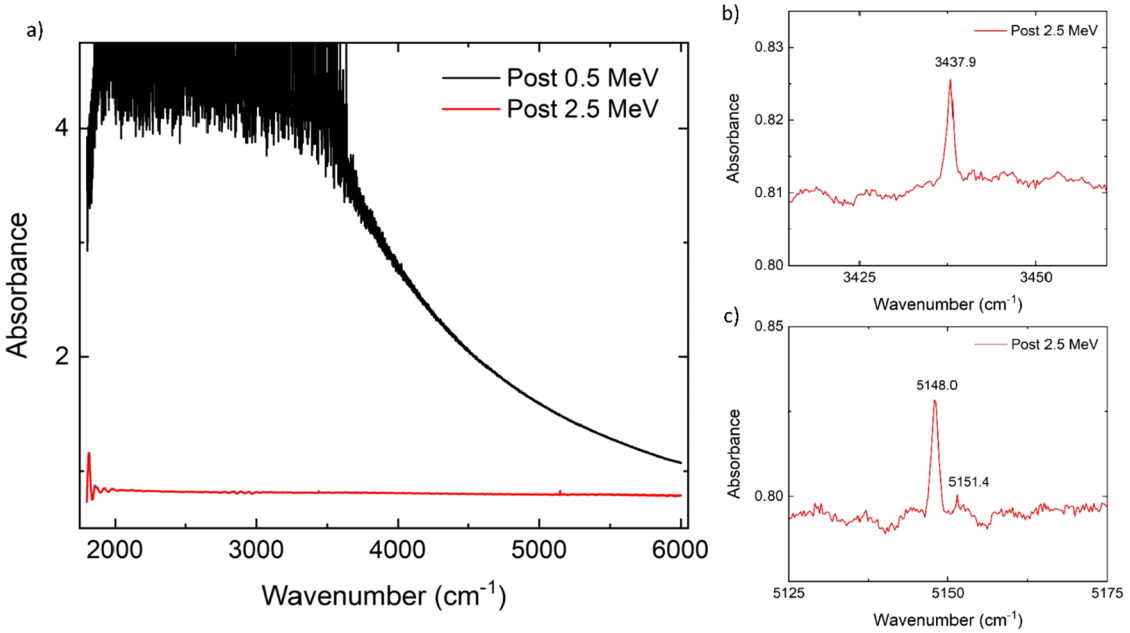

FIG. 2. (a) Low-temperature IR absorbance spectra of Hf-doped β-Ga_2O_3 samples post-electron irradiation with 0.5 and 2.5 MeV energy. The absorbance was calculated using a blank spectrum (no sample) as the baseline. (b) Spectrum of the 2.5 MeV irradiated sample showing an O–H vibrational peak. (c) Spectrum of the 2.5 MeV irradiated sample showing Ir^{4+} electronic transitions.

red luminescence.[31,32] Cr^{3+} in β-Ga_2O_3 has defect absorption bands at 430 nm (2.88 eV) and 600 nm (2.07 eV), corresponding to $^4A_2 \rightarrow {}^4T_1$ and $^4A_2 \rightarrow {}^4T_2$ transitions, respectively.[25,31,33–36] The Cr^{3+} emission spectrum in β-Ga_2O_3 consists of two sharp peaks, the *R*-lines, at 689 nm (1.80 eV) and 696 nm (1.78 eV) with a broad red peak around 715 nm (~1.7 eV). The $^2E \rightarrow {}^4A_2$ and $^4T_2 \rightarrow {}^4A_2$ internal Cr^{3+} transitions are responsible for the sharp and broad peaks, respectively.[25,33–38]

II. EXPERIMENTAL

Monoclinic single crystals used in this work were grown at the Washington State University Institute of Materials Research via the Czochralski (CZ) technique.[26,39–46] Hf-doped β-Ga_2O_3 single crystals with 0.25 at. % Hf were grown via CZ, as reported by Saleh *et al.*[40] Zn-doped β-Ga_2O_3 single crystals with 0.25 at. % Zn were grown via CZ, as reported by Jesenovec *et al.*[41] The samples

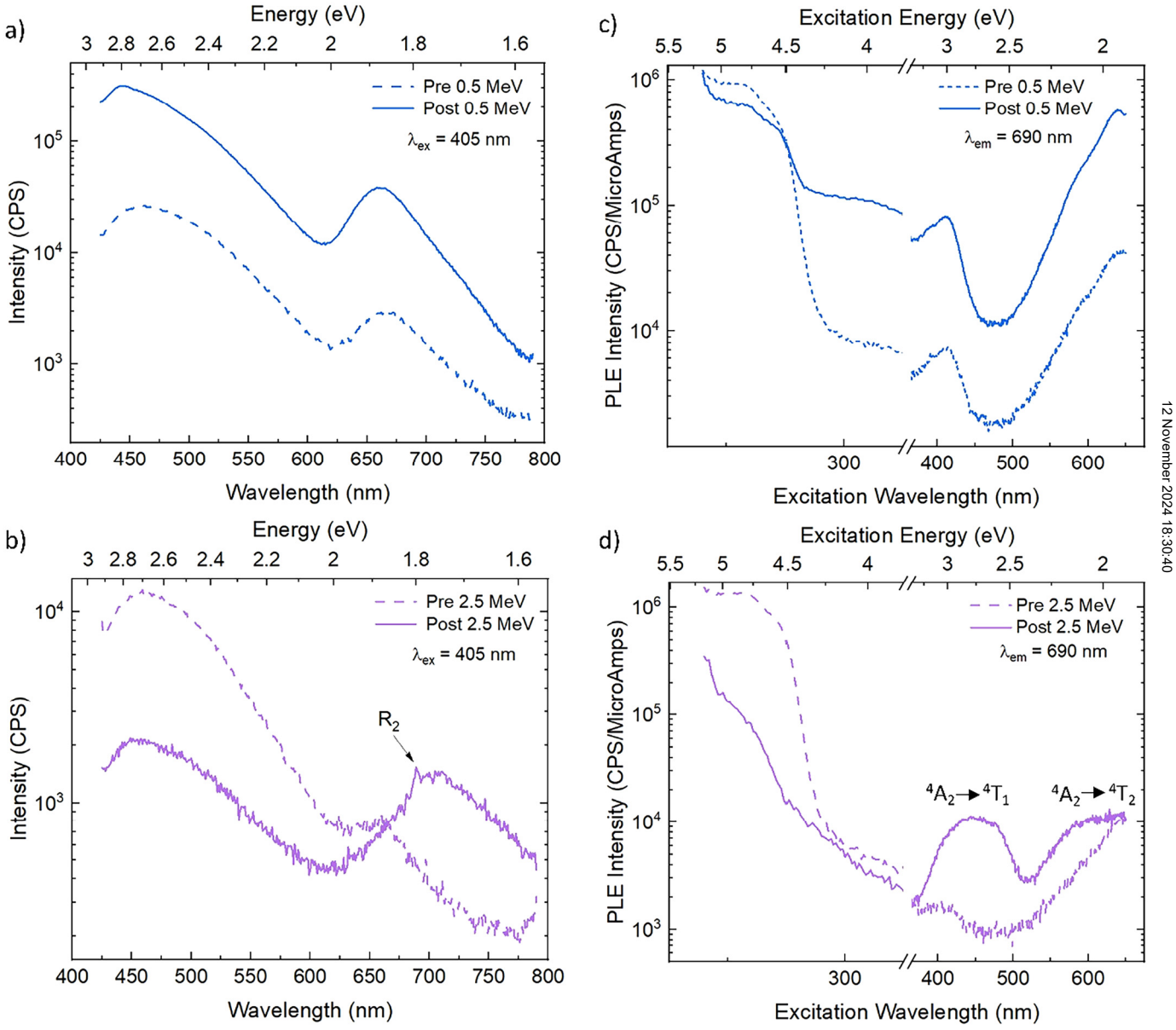

FIG. 3. PL spectra at 405 nm excitation of Hf-doped β-Ga_2O_3 pre- and post- (a) 0.5 and (b) 2.5 MeV irradiation. Corresponding PLE spectra at 690 nm emission are shown in (c) and (d). CPS = counts per second.

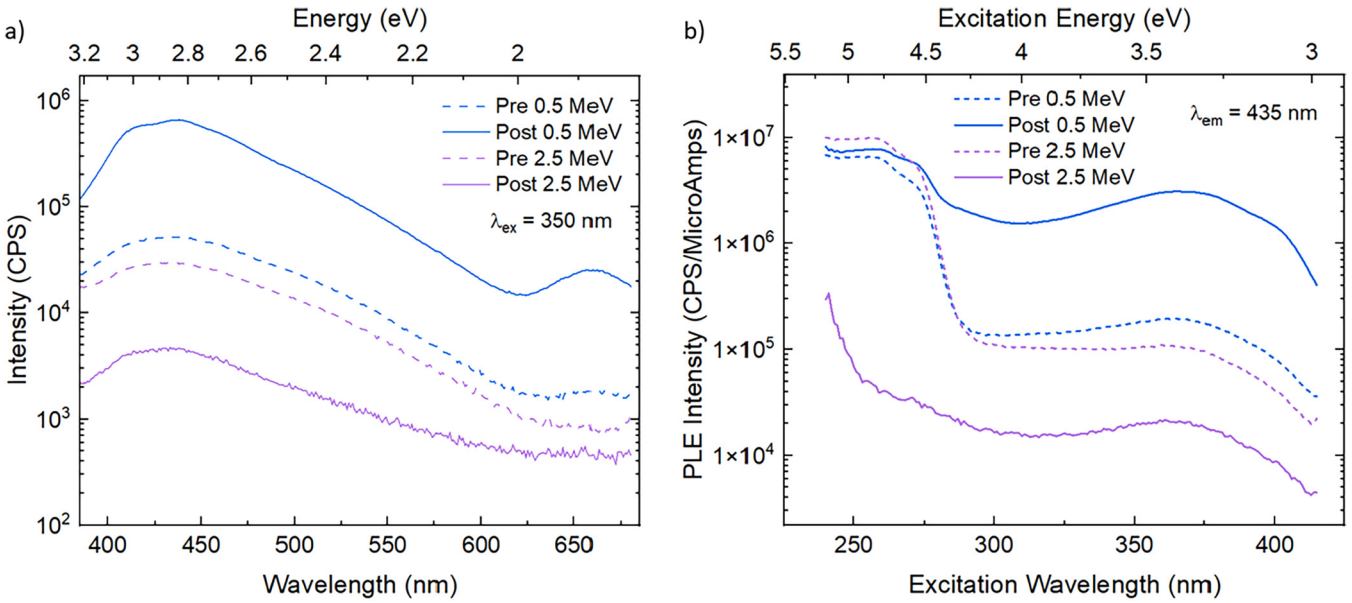

FIG. 4. (a) PL spectra at 350 nm excitation of Hf-doped β-Ga_2O_3 pre- and post-0.5 and -2.5 MeV irradiation. (b) PLE spectra at 435 nm emission.

selected from the Hf-doped growth were from the vertical gradient freeze (VGF) boule, which is the portion of the crystal that remains in the crucible after the CZ growth process. The samples from the Zn-doped growth were from the pulled CZ boule. Sample thicknesses were 0.34–1.6 mm.

2.5 and 0.5 MeV electron irradiation was performed at the SIRIUS electron accelerator facility at LSI (Laboratoire des Solides Irradiés), Palaiseau, France. Two different dose and energy conditions were performed. The first irradiation was 0.5 MeV, 1.00×10^{18} e^-/cm^2 at 23 °C with 2.28×10^{13} $e^-/(cm^2 s)$, and

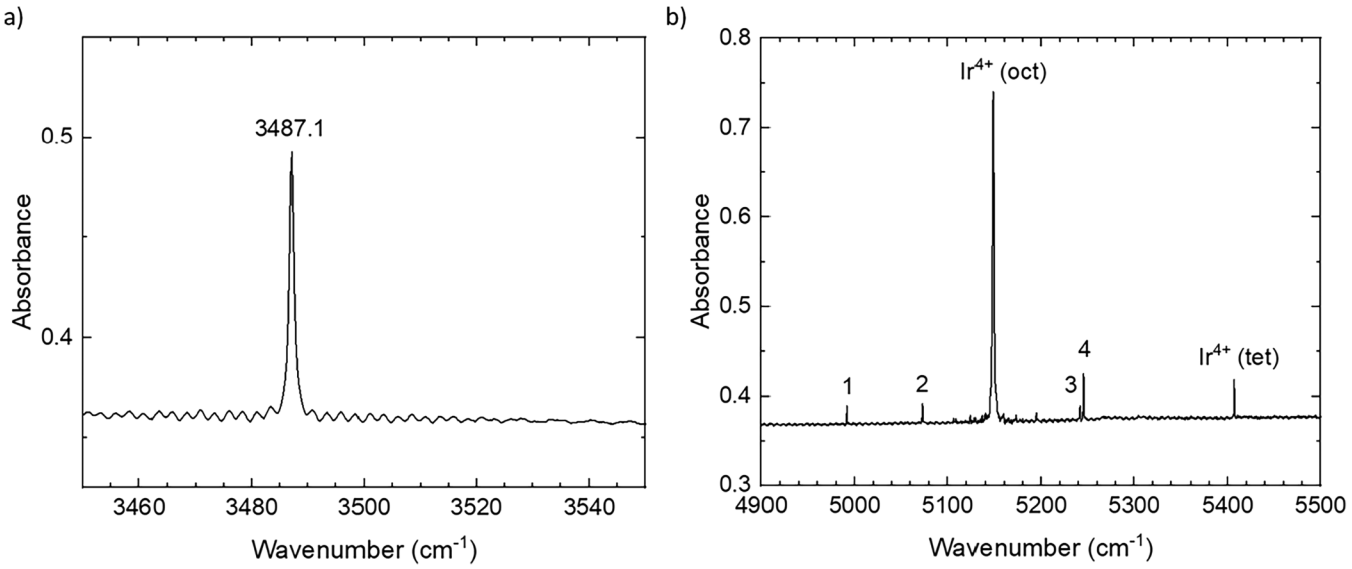

FIG. 5. Low-temperature IR spectra of Zn-doped β-Ga_2O_3 sample post-electron irradiation with 0.5 MeV energy. The absorbance was calculated using a blank spectrum as the baseline. (a) IR absorption spectrum of the ZnH complex. (b) IR absorption spectra of Ir^{4+} electronic transitions.

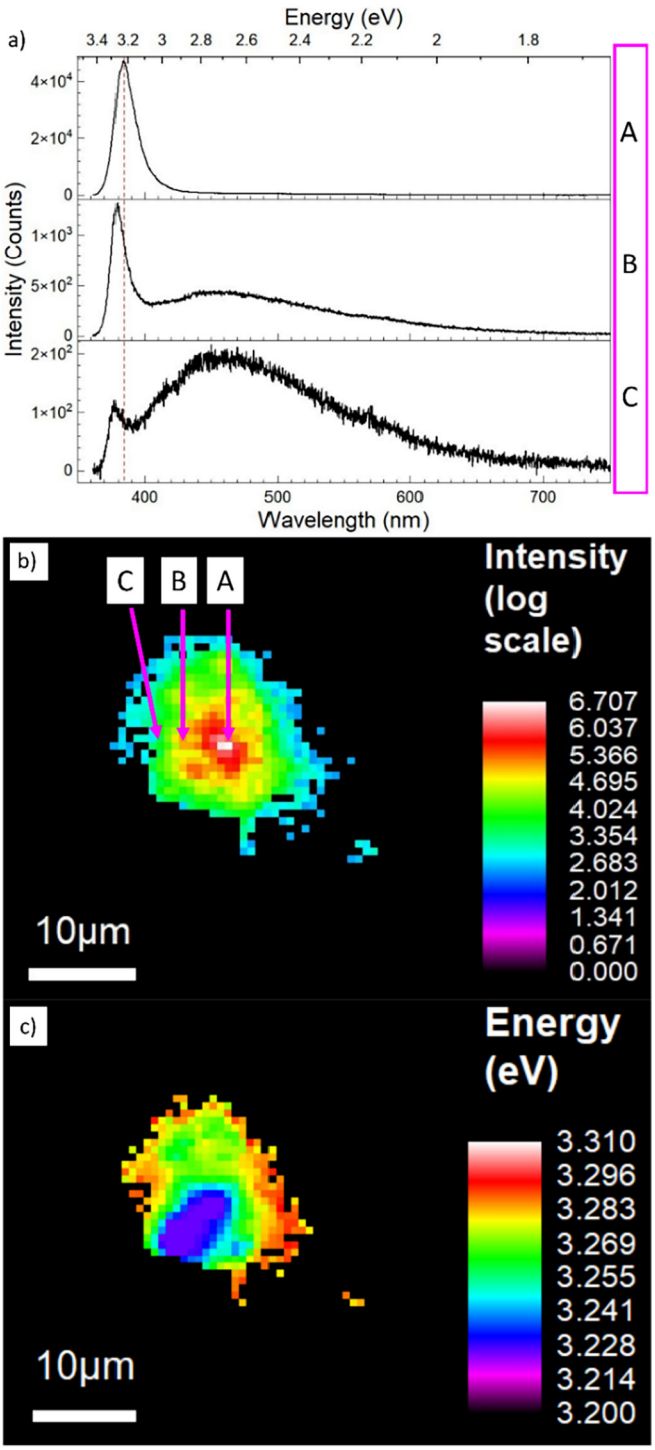

FIG. 6. (a) PL spectra (355 nm excitation) of an as-grown β-Ga_2O_3:Zn sample showing different locations on a ZnO precipitate. (b) False color map of the UV PL emission intensity, with three locations labeled. (c) False color map showing PL energy.

penetrating ~1 mm into a sample. The second irradiation was 2.5 MeV, 1.007×10^{19} e^-/cm^2 at 29 °C with 2.85×10^{13} $e^-/(cm^2 s)$, and penetrating throughout the bulk of the sample. Measurements on samples were performed on the same face that was incident to the electron beam.

The as-grown and 0.5 MeV irradiated Ga_2O_3:Zn samples had thicknesses of 1.61 and 1.07 mm, respectively. Because the sample thickness of 1.07 mm is close to the penetration depth of ~1 mm for 0.5 MeV electrons, it is possible that the bulk measurements were affected by a high concentration of defects at the stopping range. However, for the Hf-doped samples, the thicknesses of the 0.5 MeV electron-irradiated, 2.5 MeV electron-irradiated, and the as-grown comparison samples were 0.49, 0.34, and 0.94 mm, respectively. Hence, the Hf-doped samples are less likely to have been affected by the stopping range of electrons.

Two-point resistance measurements were performed on the Hf-doped samples with pressed indium contacts. A Keithley 2400 Digital Multimeter was used for an as-grown sample and 0.5 MeV irradiated sample, while the highly resistive 2.5 MeV irradiated sample was measured with a Keithley Instruments 6487 Picoammeter. The as-grown, 0.5 MeV, and 2.5 MeV irradiated samples had measured resistance values of approximately 10 Ω, 60 kΩ, and 500 GΩ, respectively.

Infrared transmission measurements were performed with a Bomem DA8 vacuum Fourier transform infrared (FTIR) spectrometer using a SiC source, KBr beam splitter, and InSb detector. Spectra were collected at 10 K with a resolution of 0.5 cm^{-1}. Ultraviolet-Visible (UV-Vis) transmission measurements were performed under ambient conditions using a Perkin Elmer Lambda 900 Series UV-Vis spectrometer.

Photoluminescence (PL) and photoluminescence excitation (PLE) spectra were measured by a Horiba Jobin-Yvon FluoroLog-3 spectrometer with double-grating monochromators and a photomultiplier tube. The excitation source is a broadband 450 W xenon continuous-wave gas discharge lamp. Excitation wavelengths from 240 to 600 nm were selected by passing light through a monochromator. While PL spectra show emission for specific excitation, the PLE measurement collects light emitted at a specified wavelength and plots the intensity of this emission vs excitation wavelength. For FTIR and UV-Vis measurements, light was incident perpendicular to the (100) surface. For PL and PLE, the light was incident at an ~30° angle to the (100) plane of the crystal. These PL and PLE spectra were acquired for a pristine sample pre-irradiation and then on the same sample post-irradiation. (For the other measurements, an as-grown sample from the same growth run was used as the reference.)

PL mapping was carried out on the (100) face using a Klar Mini Pro microscope with 355 nm laser excitation. An Ocean Optics spectrometer was selected to cover the spectral region of interest. High-resolution maps were collected using a spatial step size of 0.7 μm, while large-scale maps of the sample used a step size of 3 μm. Spectral fitting was performed using Graphics Processing Unit (GPU) accelerated fitting. A custom model consisting of Gaussian and bi-Gaussian functions was used to match the observed spectral features of the sample. Maps of the fitted spectral parameters were then plotted as false-color images.

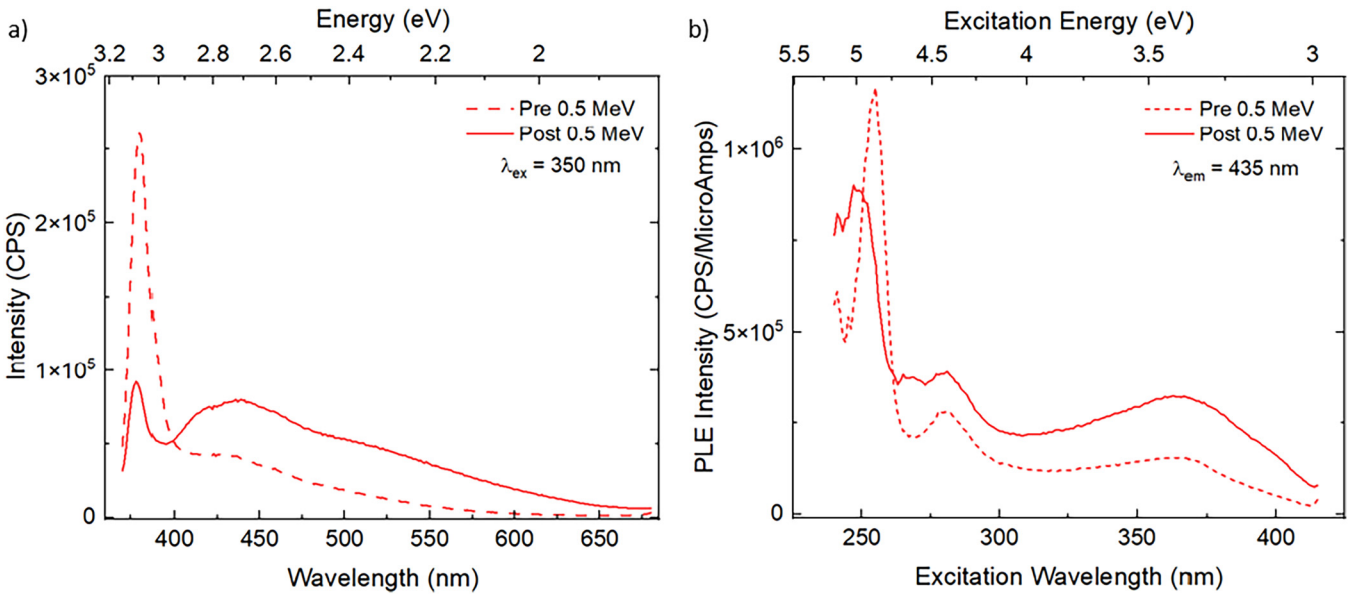

FIG. 7. (a) PL spectra at 350 nm excitation of Zn-doped β-Ga_2O_3 pre- and post-0.5 MeV irradiation. (b) PLE spectra at 435 nm emission.

III. RESULTS AND DISCUSSION

A. Hf-doped β-Ga_2O_3 color and conductivity change

The electron-irradiated Hf-doped sample that received the highest energy irradiation (2.5 MeV) experienced a drastic color change from blue to yellow [Fig. 1(a)]. Irradiation with electrons of 2.5 MeV has been reported to create mostly acceptor-like gallium vacancies and/or vacancy complexes.[14,27] This claim is supported by the fact that the yellowed sample became electrically insulating, consistent with the formation of V_{Ga} acceptors. These point defects absorb in the blue part of the visible spectrum [Fig. 1(b)], giving rise to the yellow color.[1,47,48]

The sample that received 0.5 MeV irradiation showed a minimal color change compared to the as-grown sample. As discussed previously, simulations indicate that electron irradiation with a lower energy (0.5 MeV) primarily creates oxygen vacancies.[14] The as-grown (not shown) and 0.5 MeV [Fig. 2(a)] samples demonstrated free carrier absorption, consistent with the creation of oxygen vacancies, which act as deep donors and, therefore, should not affect the *n*-type conductivity,[1,14,47,49,50] Gallium vacancies, which can compensate donors, were apparently not formed at a high enough concentration at 0.5 MeV to suppress free-carrier absorption. The 2.5 MeV sample, in contrast, showed no free carrier absorption. This large reduction in free carrier concentration is likely due to the compensation of electrically active Hf donors.

The creation of V_{Ga} defects is further supported by the presence of the V_{Ga}2H peak (3437.9 cm^{-1}),[51] which was observed after irradiation without deliberate hydrogenation. The dominant Ir^{4+} peak at 5148.0 cm^{-1} [Fig. 2(c)] has been assigned to an internal electronic transition of an isolated Ir^{4+} atom on an octahedral Ga(II) site.[52–56] The presence of the +4 oxidation state is consistent with the Ir donor compensating deep V_{Ga} acceptors or V_{Ga} complexes. We tentatively attribute the small sideband peak at 5151.4 cm^{-1} to an Ir^{4+}-V_{Ga} pair.

The PL emission spectrum post-2.5 MeV showed peaks due to Cr^{3+} impurities in β-Ga_2O_3. The R_2 line at 689 nm (1.80 eV) is visible; however, the R_1 line at 696 nm (1.78 eV) is difficult to observe due to its low intensity [Fig. 3(a)].[33–35] Correspondingly, PLE showed defect absorption bands at 430 nm (2.9 eV) and 600 nm (2.0 eV) [Fig. 3(b)]. These are assigned to Cr^{3+} absorption in β-Ga_2O_3.[31] In comparison, the 0.5 MeV sample showed no Cr^{3+} emission features or absorption bands. This confirms that Cr^{3+} can be an indicator of the Fermi level.[22,25,26] In this case, as-grown Hf-doped β-Ga_2O_3 has a Fermi level near the conduction band minimum, so the Cr^{2+} charge state may be more prevalent, but for more insulating β-Ga_2O_3, there is stronger Cr^{3+} absorption. The increased Cr^{3+} population can be explained by the shifting of the Fermi level toward the middle of the bandgap due to the creation of V_{Ga} acceptors during irradiation.[14]

A blue emission band was also seen for all materials with 350 nm excitation [Fig. 4(a)]. Blue emissions, common for β-Ga_2O_3, have been attributed to donor–acceptor pairs where the donors are oxygen vacancies.[57–60] The broad blue emission (435 nm) was much stronger for the sample irradiated with 0.5 MeV electrons, which supports the model that oxygen vacancy donors are involved. There is a PLE absorption band around 370 nm [Fig. 4(b)] that is associated with the blue emission. For photon energies near and above the bandgap (>4.5 eV), the emission intensity increases further.

B. Zn-doped β-Ga_2O_3

There were no significant differences between the IR absorption spectra observed for the 0.5 MeV irradiated sample compared

to the as-grown Zn-doped sample.[52] The crystals were yellow in color before and after the irradiation process due to absorption by Ir^{4+} impurities.[54]

The 3487 cm^{-1} peak is due to an ^{16}O–H mode of the ZnH complex.[52] There is no $V_{Ga}2H$ peak (3437.9 cm^{-1}).[51] The dominant Ir^{4+} peak at 5147.6 cm^{-1} is attributed to an internal electronic transition, while sideband peaks at 4991.0, 5072.5, 5241.2, and 5245.0 cm^{-1} [numbered 1–4 in Fig. 5(b)] were attributed to Ir^{4+} paired with Zn on a Ga(I) site.[52] A smaller peak at 5406.3 cm^{-1} [Fig. 5(b)] has been assigned to an isolated Ir^{4+} atom on a tetrahedral Ga(I) site.[52]

Room-temperature PL maps of an as-grown Zn-doped β-Ga_2O_3 sample (Fig. 6) showed precipitates with a strong ZnO band-edge peak at 384 nm (3.23 eV) and a broad defect emission feature centered around 460 nm (2.7 eV).[61] Similar spectra have been observed in ZnO powder,[62] and the PL peak near 384 nm has been attributed to stacking faults.[63,64] Figures 6(b) and 6(c) illustrate the intensity and energy maps of one of these precipitates. Figure S4 in the supplementary material shows a PL map across a larger sample surface area.

The brightest 384 nm emission was found to be in the center of the precipitate, labeled as A in Figs. 6(b) and 6(c). The intensity of this emission decreases radially outward and blue-shifts from 384 to 377 nm (3.29 eV), indicating a drop in stacking-fault PL. At the same time, the 460 nm emission becomes more prominent relative to the band-edge PL. This spatial variation suggests that the outer shell, labeled as C, contains more point defects, which result in 460 nm emission, than the interior core (A). The common "green luminescence" in ZnO single crystals and powders[65,66] was not observed here.

To investigate the effect of electron irradiation, non-spatially resolved PL spectra were collected (Fig. 7). These spectra comprise an average of many precipitates and variations within each precipitate. Therefore, the band-edge emission peaks at 380 nm rather than 384 nm. 0.5 MeV irradiation leads to quenching of the band-edge ZnO PL and a blue-shift from 380 to 377 nm. This indicates an overall reduction in the stacking-fault PL, similar to the "shell" in the as-grown precipitate.

As discussed previously, the β-Ga_2O_3 broad blue emission band was enhanced for the sample irradiated with 0.5 MeV electrons (Fig. 4). The increase in blue emission is likely the result of oxygen vacancy formation in β-Ga_2O_3. A similar PLE absorption band to that of the Hf-doped sample is seen around 370 nm [Figs. 4(b) and 7(b)], along with an additional near band-edge (280 nm) feature.

PL maps of the ZnO precipitates in the 0.5 MeV irradiated β-Ga_2O_3:Zn sample correlated with what was observed with the spatially averaged PL. Emission energy was brightest in the core, labeled as A in Figs. 8(b) and 8(c), and was found to be closer to 379 nm. The intensity of this emission also decreases radially outward and blue-shifts from 379 to 376 nm. The emission that was previously centered around 460 nm is now broader and centered around 520 nm. Like the as-grown sample, this broad emission band becomes more prominent relative to the band-edge PL going from the core to the shell. Overall, electron irradiation appears to increase the density of point defects throughout the precipitate.

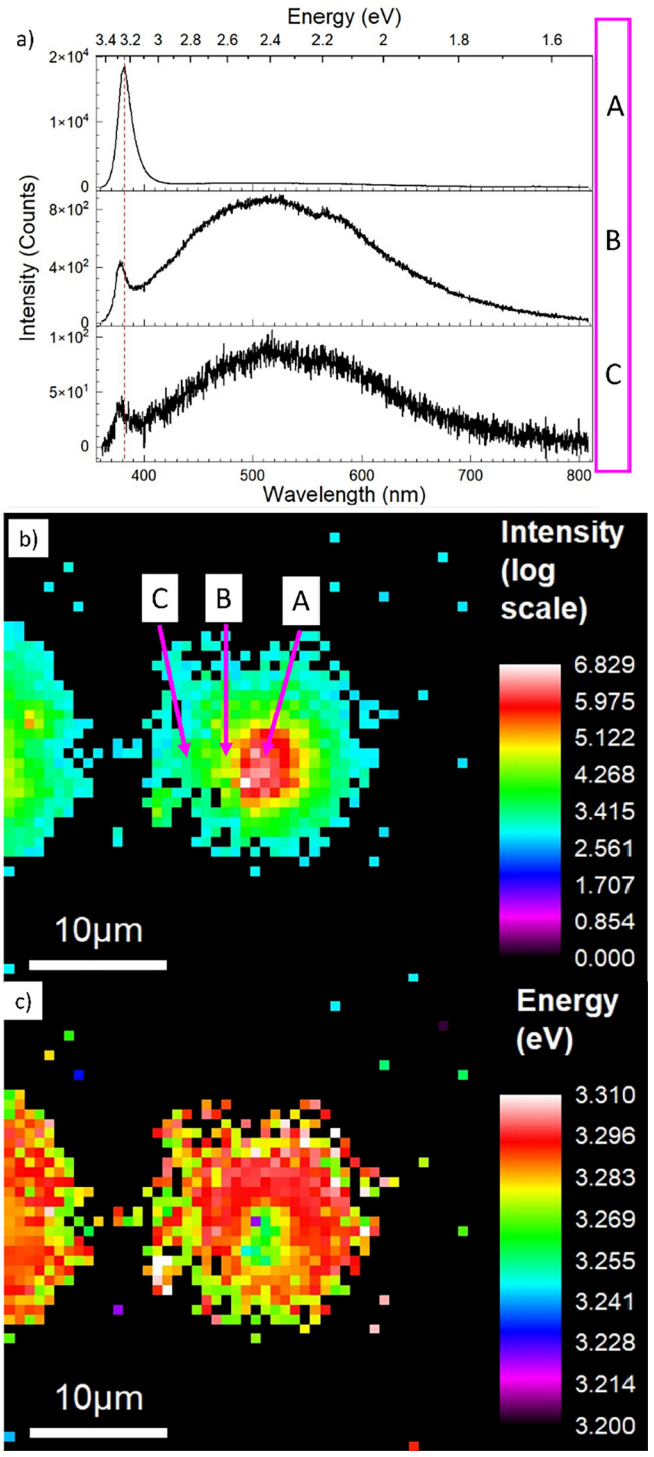

FIG. 8. (a) PL spectra (355 nm excitation) of the 0.5 MeV irradiated β-Ga_2O_3:Zn sample showing different locations on a ZnO precipitate. (b) False color map of the UV PL intensity, with three locations labeled. (c) False color map showing the PL energy.

IV. CONCLUSIONS

In this work, the optical properties of *n*-type and insulating β-Ga_2O_3 samples were altered via high-energy electron irradiation, directly impacting photoluminescence and transmission spectra. The 2.5 MeV irradiated β-Ga_2O_3:Hf sample experienced a drastic color and conductivity change that may be due to the creation of gallium vacancies, which compensated carriers from the Hf donors. This resulted in the absence of free-carrier absorption seen by IR as well as the presence of Cr^{3+} emissions and absorption due to the shifted Fermi level. Blue PL was enhanced, which correlates the increase in oxygen vacancy concentration for the 0.5 MeV irradiated samples.

We also observed optically active ZnO precipitates that form during growth of β-Ga_2O_3:Zn. Spatially averaged PL indicate that the band-edge 380 nm ZnO emission was quenched with 0.5 MeV irradiation and blue-shifted toward 377 nm. A similar band-edge, core–shell structure was seen for the as-grown and irradiated samples. Electron irradiation resulted in a blue shift of the band-edge peak and a prominent blue-green emission band, suggesting that 0.5 MeV irradiation increased the point defect population in the ZnO precipitates.

SUPPLEMENTARY MATERIAL

See the supplementary material for sample information and additional spectra.

ACKNOWLEDGMENTS

The authors would like to thank Corey Halverson for assistance with electron irradiation experiment. Jackie Cooke and Mike Scarpulla (University of Utah) are gratefully acknowledged for helpful discussions related to PL. This work was supported by Air Force Office of Scientific Research under Award No. FA9550-21-1-0078 monitored by Dr. Ali Sayir. Additional support was provided by the U.S. Department of Energy, Office of Basic Energy Sciences, Division of Materials Science and Engineering under Award No. DE-FG02-07ER46386 (M.D.M.). Jani Jesenovec and Muad Saleh were the crystal growers for the Zn-and Hf-doped samples, respectively.

AUTHOR DECLARATIONS

Conflict of Interest

J.H. is an employee of Klar Scientific, and M.D.M. owns equity in the company.

Author Contributions

Cassandra Remple: Conceptualization (equal); Formal analysis (lead); Investigation (lead); Writing – original draft (lead); Writing – review & editing (lead). **Jesse Huso:** Investigation (equal); Writing – review & editing (equal). **Marc H. Weber:** Investigation (equal). **John S. McCloy:** Conceptualization (equal); Funding acquisition (equal); Investigation (equal); Project administration (equal); Writing – review & editing (equal). **Matthew D. McCluskey:** Conceptualization (equal); Funding acquisition (equal); Investigation (equal); Project administration (equal); Writing – review & editing (lead).

DATA AVAILABILITY

The data that support the findings of this study are within the article and its supplementary material.

REFERENCES

[1]M. D. McCluskey, "Point defects in Ga_2O_3," J. Appl. Phys. **127**(10), 101101 (2020).
[2]M. Higashiwaki, K. Sasaki, H. Murakami, Y. Kumagai, A. Koukitu, A. Kuramata, T. Masui, and S. Yamakoshi, "Recent progress in Ga_2O_3 power devices," Semicond. Sci. Technol. **31**(3), 034001 (2016).
[3]M. J. Tadjer, "Toward gallium oxide power electronics," Science **378**(6621), 724–725 (2022).
[4]C. Kim, G. Pilania, and R. Ramprasad, "From organized high-throughput data to phenomenological theory using machine learning: The example of dielectric breakdown," Chem. Mater. **28**(5), 1304–1311 (2016).
[5]A. Kalra, U. U. Muazzam, R. Muralidharan, S. Raghavan, and D. N. Nath, "The road ahead for ultrawide bandgap solar-blind UV photodetectors," J. Appl. Phys. **131**(15), 150901 (2022).
[6]C. Venkata Prasad, M. Labed, M. T. Alam Shamim Shaikh, J. Y. Min, T. H. Vu Nguyen, W. Song, K. J. Kim, and Y. S. Rim, "Ga_2O_3-based X-ray detector and scintillators: A review," Mater. Today Phys. **35**, 101095 (2023).
[7]T. Yanagida, G. Okada, T. Kato, D. Nakauchi, and S. Yanagida, "Fast and high light yield scintillation in the Ga_2O_3 semiconductor material," Appl. Phys. Express **9**(4), 042601 (2016).
[8]N. He, X. Ouyang, M. Xu, H. Tang, B. Liu, Z. Zhu, M. Gu, J. Xu, J. Liu, and L. Chen, "Scintillation properties of β-Ga_2O_3 single crystal excited by alpha-ray," IEEE Trans. Nucl. Sci. **67**(1), 400–404 (2020).
[9]J. Kim, S. J. Pearton, C. Fares, J. Yang, F. Ren, S. Kim, and A. Y. Polyakov, "Radiation damage effects in Ga_2O_3 materials and devices," J. Mater. Chem. C **7**(1), 10–24 (2019).
[10]A. Azarov, J. G. Fernández, J. Zhao, F. Djurabekova, H. He, R. He, Ø. Prytz, L. Vines, U. Bektas, P. Chekhonin, N. Klingner, G. Hlawacek, and A. Kuznetsov, "Universal radiation tolerant semiconductor," Nat. Commun. **14**(1), 4855 (2023).
[11]B. R. Tuttle, N. J. Karom, A. O'Hara, R. D. Schrimpf, and S. T. Pantelides, "Atomic-displacement threshold energies and defect generation in irradiated β-Ga_2O_3: A first-principles investigation," J. Appl. Phys. **133**(1), 015703 (2023).
[12]K. Wang, R. Cao, B. Mei, H. Zhang, H. Lv, L. Zhao, Y. Xue, and X. Zeng, "Influence of high-dose 80 MeV proton irradiation on the electronic structure and photoluminescence of β-Ga_2O_3," J. Electron. Mater. **52**, 7718–7727 (2023).
[13]M. Peres, A. J. S. Fernandes, F. J. Oliveira, L. C. Alves, E. Alves, T. S. Monteiro, S. Cardoso, M. Alonso-Orts, E. Nogales, B. Méndez, E. G. Víllora, K. Shimamura, and K. Lorenz, "Micro-opto-electro-mechanical device based on flexible β-Ga_2O_3 micro-lamellas," ECS J. Solid State Sci. Technol. **8**(7), Q3235–Q3241 (2019).
[14]A. Alessi, O. Cavani, R. Grasset, H.-J. Drouhin, V. I. Safarov, and M. Konczykowski, "Electron irradiation: From test to material tailoring," Europhys. Lett. **143**(5), 56001 (2023).
[15]T.-H. Dang, M. Konczykowski, V. I. Safarov, E. Hammou, L. Romero Vega, N. Ollier, R. Grasset, A. Alessi, H.-J. M. Drouhin, H. Jaffrès, V. Y. Davydov, A. Wołoś, D. J. Rogers, V. E. Sandana, P. Bove, and F. H. Teherani, in *Oxide-Based Materials and Devices XIII*, edited by F. H. Teherani and D. J. Rogers (SPIE, San Francisco, 2022), p. 60.
[16]T.-H. Dang, M. Konczykowski, H. Jaffrès, V. I. Safarov, and H.-J. Drouhin, "Modification of β-gallium oxide electronic properties by irradiation with high-energy electrons," J. Vac. Sci. Technol. A **40**(3), 033416 (2022).
[17]N. F. Mott, "The scattering of fast electrons by atomic nuclei," Proc. R. Soc. Lond. Ser. A **124**(794), 425–442 (1929).

[18]C. Zimmermann, E. F. Verhoeven, Y. K. Frodason, P. M. Weiser, J. B. Varley, and L. Vines, "Formation and control of the E* center in implanted β-Ga_2O_3 by reverse-bias and zero-bias annealing," J. Phys. Appl. Phys. **53**(46), 464001 (2020).
[19]E. Farzana, M. F. Chaiken, T. E. Blue, A. R. Arehart, and S. A. Ringel, "Impact of deep level defects induced by high energy neutron radiation in β-Ga_2O_3," APL Mater. **7**(2), 022502 (2018).
[20]D. S. Billington and J. H. Crawford, *Radiation Damage in Solids* (Princeton University Press, Princeton, NJ, 1961).
[21]J. R. Srour, C. J. Marshall, and P. W. Marshall, "Review of displacement damage effects in silicon devices," IEEE Trans. Nucl. Sci. **50**(3), 653–670 (2003).
[22]M. Peres, D. M. Esteves, B. M. S. Teixeira, J. Zanoni, L. C. Alves, E. Alves, L. F. Santos, X. Biquard, Z. Jia, W. Mu, J. Rodrigues, N. A. Sobolev, M. R. Correia, T. Monteiro, N. Ben Sedrine, and K. Lorenz, "Enhancing the luminescence yield of Cr^{3+} in β-Ga_2O_3 by proton irradiation," Appl. Phys. Lett. **120**(26), 261904 (2022).
[23]K. Cho, M. Kończykowski, S. Teknowijoyo, M. A. Tanatar, and R. Prozorov, "Using electron irradiation to probe iron-based superconductors," Supercond. Sci. Technol. **31**(6), 064002 (2018).
[24]E. Wendler, E. Treiber, and J. Baldauf, in *11th International Conference on Interaction Radiation Solids* (Belarusian State University, 2015), p. 93.
[25]V. Vasyltsiv, A. Luchechko, Y. Zhydachevskyy, L. Kostyk, R. Lys, D. Slobodzyan, R. Jakieła, B. Pavlyk, and A. Suchocki, "Correlation between electrical conductivity and luminescence properties in β-Ga_2O_3:Cr^{3+} and β-Ga_2O_3:Cr,Mg single crystals," J. Vac. Sci. Technol. A **39**(3), 033201 (2021).
[26]J. Jesenovec, B. L. Dutton, C. Remple, N. Smith-Gray, M. Murugesan, C. Peterson, B. K. Downing, S. Krishnamoorthy, M. D. McCluskey, and J. S. McCloy, "Alternative alloy to increase bandgap in gallium oxide, β-$(Sc_xGa_{1-x})_2O_3$, and rare earth stark luminescence," J. Cryst. Growth **596**, 126823 (2022).
[27]B. E. Kananen, L. E. Halliburton, K. T. Stevens, G. K. Foundos, and N. C. Giles, "Gallium vacancies in β-Ga_2O_3 crystals," Appl. Phys. Lett. **110**(20), 202104 (2017).
[28]A. Kuramata, K. Koshi, S. Watanabe, Y. Yamaoka, T. Masui, and S. Yamakoshi, "High-quality β-Ga_2O_3 single crystals grown by edge-defined film-fed growth," Jpn. J. Appl. Phys. **55**(12), 1202A2 (2016).
[29]A. Luchechko, V. Vasyltsiv, Y. Zhydachevskyy, M. Kushlyk, S. Ubizskii, and A. Suchocki, "Luminescence spectroscopy of Cr^{3+} ions in bulk single crystalline β-Ga_2O_3," J. Phys. Appl. Phys. **53**(35), 354001 (2020).
[30]D. Vivien, B. Viana, A. Revcolevschi, J. D. Barrie, B. Dunn, P. Nelson, and O. M. Stafsudd, "Optical properties of β-Ga_2O_3:Cr^{3+} single crystals for tunable laser applications," J. Lumin. **39**(1), 29–33 (1987).
[31]H. H. Tippins, "Optical and microwave properties of trivalent chromium in β-Ga_2O_3," Phys. Rev. **137**(3A), A865–A871 (1965).
[32]Y. Tanabe and S. Sugano, "On the absorption spectra of complex ions. I," J. Phys. Soc. Jpn. **9**(5), 753–766 (1954).
[33]Y. Tokida and S. Adachi, "Photoluminescence spectroscopy and energy-level analysis of metal-organic-deposited Ga_2O_3:Cr^{3+} films," J. Appl. Phys. **112**(6), 063522 (2012).
[34]R. Sun, Y. K. Ooi, P. T. Dickens, K. G. Lynn, and M. A. Scarpulla, "On the origin of red luminescence from iron-doped β-Ga_2O_3 bulk crystals," Appl. Phys. Lett. **117**(5), 052101 (2020).
[35]C. Remple, L. M. Barmore, J. Jesenovec, J. S. McCloy, and M. D. McCluskey, "Photoluminescence spectroscopy of Cr^{3+} in β-Ga_2O_3 and $(Al_{0.1}Ga_{0.9})_2O_3$," J. Vac. Sci. Technol. A **41**(2), 022702 (2023).
[36]C. Remple, J. Huso, and M. D. McCluskey, "Photoluminescence and Raman mapping of β-Ga_2O_3," AIP Adv. **11**(10), 105006 (2021).
[37]C. G. Walsh, J. F. Donegan, T. J. Glynn, G. P. Morgan, G. F. Imbusch, and J. P. Remeika, "Luminescence from β-Ga_2O_3:Cr^{3+}," J. Lumin. **40–41**, 103–104 (1988).
[38]J. E. Stehr, M. Jansson, D. M. Hofmann, J. Kim, S. J. Pearton, W. M. Chen, and I. A. Buyanova, "Magneto-optical properties of Cr^{3+} in β-Ga_2O_3," Appl. Phys. Lett. **119**(5), 052101 (2021).
[39]M. Saleh, A. Bhattacharyya, J. B. Varley, S. Swain, J. Jesenovec, S. Krishnamoorthy, and K. Lynn, "Electrical and optical properties of Zr doped β-Ga_2O_3 single crystals," Appl. Phys. Express **12**(8), 085502 (2019).
[40]M. Saleh, J. B. Varley, J. Jesenovec, A. Bhattacharyya, S. Krishnamoorthy, S. Swain, and K. Lynn, "Degenerate doping in β-Ga_2O_3 single crystals through Hf-doping," Semicond. Sci. Technol. **35**(4), 04LT01 (2020).
[41]J. Jesenovec, J. Varley, S. E. Karcher, and J. S. McCloy, "Electronic and optical properties of Zn-doped β-Ga_2O_3 Czochralski single crystals," J. Appl. Phys. **129**(22), 225702 (2021).
[42]J. Jesenovec, C. Remple, J. Huso, B. Dutton, P. Toews, M. D. McCluskey, and J. S. McCloy, "Photodarkening and dopant segregation in Cu-doped β-Ga_2O_3 Czochralski single crystals," J. Cryst. Growth **578**, 126419 (2021).
[43]J. Jesenovec, C. Pansegrau, M. D. McCluskey, J. S. McCloy, T. D. Gustafson, L. E. Halliburton, and J. B. Varley, "Persistent room-temperature photodarkening in Cu-doped β-Ga_2O_3," Phys. Rev. Lett. **128**(7), 077402 (2022).
[44]J. S. McCloy, J. Jesenovec, B. Dutton, C. Pansegrau, C. Remple, M. H. Weber, S. Swain, M. McCluskey, and M. Scarpulla, in *Oxide-Based Materials and Devices XIII*, edited by F. H. Teherani and D. J. Rogers (SPIE, San Francisco, 2022), p. 10.
[45]J. Jesenovec, B. Dutton, N. Stone-Weiss, A. Chmielewski, M. Saleh, C. Peterson, N. Alem, S. Krishnamoorthy, and J. S. McCloy, "Alloyed β-$(Al_xGa_{1-x})_2O_3$ bulk Czochralski single β-$(Al_{0.1}Ga_{0.9})_2O_3$ and polycrystals β-$(Al_{0.33}Ga_{0.66})_2O_3$, β-$(Al_{0.5}Ga_{0.5})_2O_3$), and property trends," J. Appl. Phys. **131**(15), 155702 (2022).
[46]B. L. Dutton, C. Remple, J. Jesenovec, S. Ghandiparsi, M. S. Gottlieb, J. B. Varley, L. F. Voss, M. D. McCluskey, and J. S. McCloy, in *Oxide-Based Materials and Devices XIV*, edited by F. H. Teherani and D. J. Rogers (SPIE, San Francisco, 2023), p. 17.
[47]Z. Galazka, "Growth of bulk β-Ga_2O_3 single crystals by the Czochralski method," J. Appl. Phys. **131**(3), 031103 (2022).
[48]E. Korhonen, F. Tuomisto, D. Gogova, G. Wagner, M. Baldini, Z. Galazka, R. Schewski, and M. Albrecht, "Electrical compensation by Ga vacancies in Ga_2O_3 thin films," Appl. Phys. Lett. **106**(24), 242103 (2015).
[49]J. B. Varley, J. R. Weber, A. Janotti, and C. G. Van de Walle, "Oxygen vacancies and donor impurities in β-Ga_2O_3," Appl. Phys. Lett. **97**(14), 142106 (2010).
[50]M. Yamaga, E. G. Víllora, K. Shimamura, N. Ichinose, and M. Honda, "Donor structure and electric transport mechanism in β-Ga_2O_3," Phys. Rev. B **68**(15), 155207 (2003).
[51]P. Weiser, M. Stavola, W. B. Fowler, Y. Qin, and S. Pearton, "Structure and vibrational properties of the dominant O-H center in β-Ga_2O_3," Appl. Phys. Lett. **112**(23), 232104 (2018).
[52]C. Pansegrau, J. Jesenovec, J. S. McCloy, and M. D. McCluskey, "Zinc–hydrogen and zinc–iridium pairs in β-Ga_2O_3," Appl. Phys. Lett. **119**(10), 102104 (2021).
[53]J. R. Ritter, J. Huso, P. T. Dickens, J. B. Varley, K. G. Lynn, and M. D. McCluskey, "Compensation and hydrogen passivation of magnesium acceptors in β-Ga_2O_3," Appl. Phys. Lett. **113**(5), 052101 (2018).
[54]J. R. Ritter, K. G. Lynn, and M. D. McCluskey, "Iridium-related complexes in Czochralski-grown β-Ga_2O_3," J.: Appl. Phys. **126**(22), 225705 (2019).
[55]C. A. Lenyk, N. C. Giles, E. M. Scherrer, B. E. Kananen, L. E. Halliburton, K. T. Stevens, G. K. Foundos, J. D. Blevins, D. L. Dorsey, and S. Mou, "Ir^{4+} ions in β-Ga_2O_3 crystals: An unintentional deep donor," J. Appl. Phys. **125**(4), 045703 (2019).
[56]P. Seyidov, M. Ramsteiner, Z. Galazka, and K. Irmscher, "Resonant electronic Raman scattering from Ir^{4+} ions in β-Ga_2O_3," J. Appl. Phys. **131**(3), 035707 (2022).
[57]J. Cooke, P. Ranga, J. Jesenovec, J. S. McCloy, S. Krishnamoorthy, M. A. Scarpulla, and B. Sensale-Rodriguez, "Effect of extended defects on photoluminescence of gallium oxide and aluminum gallium oxide epitaxial films," Sci. Rep. **12**(1), 3243 (2022).
[58]K. Shimamura, E. G. Víllora, T. Ujiie, and K. Aoki, "Excitation and photoluminescence of pure and Si-doped—Ga_2O_3 single crystals," Appl. Phys. Lett. **92**(20), 201914 (2014).
[59]T. Onuma, Y. Nakata, K. Sasaki, T. Masui, T. Yamaguchi, T. Honda, A. Kuramata, S. Yamakoshi, and M. Higashiwaki, "Modeling and interpretation

of UV and blue luminescence intensity in β-Ga_2O_3 by silicon and nitrogen doping," J. Appl. Phys. **124**(7), 075103 (2018).
[60]S. Ohira, N. Suzuki, N. Arai, M. Tanaka, T. Sugawara, K. Nakajima, and T. Shishido, "Characterization of transparent and conducting Sn-doped β-Ga_2O_3 single crystal after annealing," Thin Solid Films **516**(17), 5763–5767 (2008).
[61]M. D. McCluskey and S. J. Jokela, "Defects in ZnO," J. Appl. Phys. **106**(7), 071101 (2009).
[62]M. Anpo and Y. Kubokawa, "Photoluminescence of zinc oxide powder as a probe of electron-hole surface processes," J. Phys. Chem. **88**(23), 5556–5560 (1984).
[63]M. Schirra, R. Schneider, A. Reiser, G. M. Prinz, M. Feneberg, J. Biskupek, U. Kaiser, C. E. Krill, K. Thonke, and R. Sauer, "Stacking fault related 3.31 eV luminescence at 130-meV acceptors in zinc oxide," Phys. Rev. B **77**(12), 125215 (2008).
[64]V. Khranovskyy, M. Sendova, B. Hosterman, N. McGinnis, I. Shtepliuk, and R. Yakimova, "Temperature dependent study of basal plane stacking faults in Ag: ZnO nanorods by Raman and photoluminescence spectroscopy," Mater. Sci. Semicond. Process. **69**, 62–67 (2017).
[65]K. Vanheusden, W. L. Warren, C. H. Seager, D. R. Tallant, J. A. Voigt, and B. E. Gnade, "Mechanisms behind green photoluminescence in ZnO phosphor powders," J. Appl. Phys. **79**(10), 7983–7990 (1996).
[66]L. S. Vlasenko and G. D. Watkins, "Optical detection of electron paramagnetic resonance in room-temperature electron-irradiated ZnO," Phys. Rev. B **71**(12), 125210 (2005).